Journal of Physics: Conference Series **1559** (2020) 012088 doi:10.1088/1742-6596/1559/1/012088

Heat extraction from HTS tape stacks applied in a superconducting motor in different cooling conditions

Lukasz Tomkow[1,a], Nikolay Mineev[1], Anis Smara[1], Vicente Climente-Alarcon[1], Bartek A. Glowacki[1,2]

[1]Applied Superconductivity and Cryoscience Group, Department of Materials Science and Metallurgy, University of Cambridge, Cambridge, United Kingdom
[2]Institute of Power Engineering, Warsaw, Poland

E-mail: [a]ltt27@cam.ac.uk

Abstract. The heat is generated inside the stack of superconducting tapes mounted on the surface of the electrical machine rotor during its operation and magnetization. Cooling of such stack presents challenges because of the layered structure of both tape, and stack. Moreover, the tapes should be electrically isolated to minimize the AC losses, that assumes gluing them, rather than soldering. The calculations consider a conductive heat dissipation also through the rotor iron.
Results show that: liquid nitrogen provides an effective cooling; the temperature of the stack shows complex distribution patterns with the gaseous coolant. Additional preventive measures were analyzed to keep the stack operational in vacuum conditions.

1. Introduction

Stacks of superconducting tapes have advantageous properties when applied as trapped-field magnets [1]. Fields as high as 17.7 T can be achieved by magnetising the stacks [2]. It is considered to apply them as permanent magnets in the rotor of a fully superconducting aircraft motor [3]. There are some limiting issues connected with such usage of the stacks. Cyclic mechanical loads present in a motor limit their critical current [4], while an external cross-field causes demagnetisation [5]. The latter issue requires the application of remagnetisation techniques [6] and the complex shapes of the stacks [7].
Removal of heat from the stacks is crucial as the increase of temperature further exacerbates magnetisation loss [8]. Different cooling conditions strongly affect achievable critical current and maximum trapped magnetic field. Different methods of thermal anchoring can change electromagnetic behaviour of the stack. Soldering it connects the tapes electrically, while glueing creates an insulating layer. Field-trapping capacity of a stack is better when its layers are separated as eddy currents formation is prevented [9]. The trade-off is that soldering provides better thermal contact and it could enhance performance of a stack by maintaining it at lower temperature despite an additional heat generation. In this paper both options are considered.
Different cooling methods can be applied. Two major options are immersion and conduction cooling [10, 11]. Immersion cooling is more efficient, but may lead to sealing problems and friction losses. These problems are decreased when operating the device in vacuum and cooling it only by conduction. In this case, though, heat extraction is limited and a significant rise of temperature may occur. Three stack cooling options are considered in this paper - cooling with

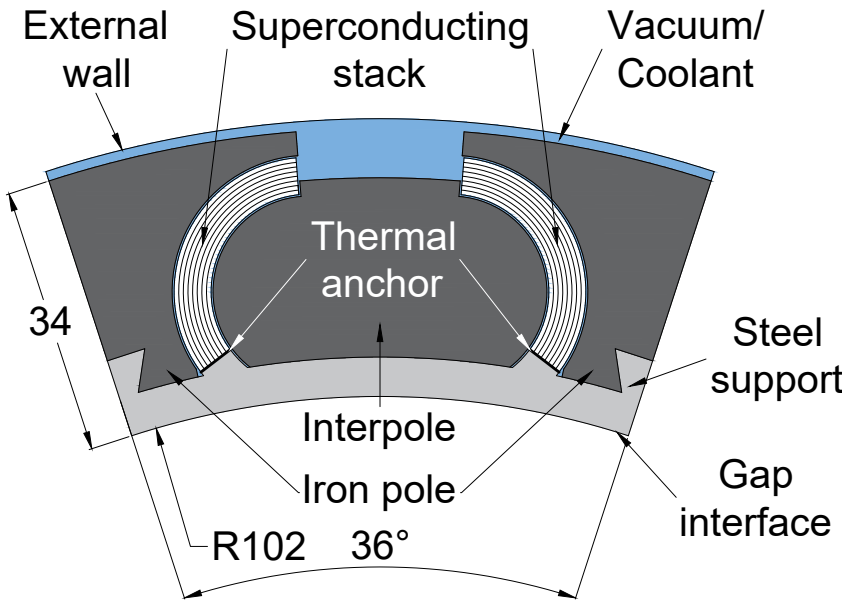

Figure 1. Geometry of the analysed section of the rotor

liquid nitrogen, gaseous helium at 20 K and maintaining the stack in vacuum.
The goal of the paper is to provide an analytical background for the selection of the best cooling method for a superconducting stack applied in an aircraft motor. The presented insights can influence the geometrical design and manufacturing of the stack to obtain the best combination of thermal and electromagnetic properties. The ultimate goal of the design of the stack is a maximum trapped magnetic field with minimum demagnetisation.

2. Methods

Geometry of the considered section of a rotor is presented in figure 1. The full rotor has five poles, each consisting of four magnetised superconducting stacks shaped as sections of rings. The tapes are placed in parallel to the surface of the stack. It is assumed that the stack is connected to rest of the rotor only at its end. Heat conduction is thus allowed only through thermal anchor to the structural steel forming the basis of the rotor.

The goal of the analysis is to find the maximum operating temperature of the stack and the time in which it is achieved. In the initial state it is assumed the temperature everywhere is the same as that of the coolant. Then heat is supplied and temperature of the system is rising. The simulation is performed until steady-state operation is reached.
The calculations are performed using Heat Transfer module of Comsol Multiphysics. In the considered 2D case with uniform initial temperatures and without considering a mass transfer the heat transfer formulas are

$$Q + q_0 = \nabla \cdot \mathbf{q} + \rho C_p \frac{\partial T}{\partial t} \tag{1}$$

$$\mathbf{q} = -\kappa \nabla T \tag{2}$$

where Q is a heat source or a heat sink, q_0 are prescribed heat fluxes, $\mathbf{q}$ is a vector field of heat transfer and T is temperature. ρ denotes density, C_p is heat capacity with constant pressure and k is a local thermal conductivity.
A fine mesh is applied to obtain high accuracy. Boundary conditions on the external walls of stack and poles depend on the modelled heat extraction method. On the sides thermal

insulations condition is always applied to reflect the symmetry of the device. Heat is assumed to be removed at the internal wall by conduction to the end of the rotor, according to formula

$$q_0 = \frac{k_{SS}(T)}{l_r} \cdot (T_s - T) \tag{3}$$

where k_{ss} is thermal conductivity of structural steel based on [12], l_r is the length of the rotor, T_s is the temperature of heat sink, assumed as the temperature of cooling medium.
The simulations in vacuum conditions assume that heat is removed only through conduction through internal boundary. The remaining walls have thermal insulation boundary imposed. This is the worst case scenario and the expected temperature rise is the highest.
The second case is heat removal with stationary helium gas. In this case it is assumed that due to small size of channels convection is negligible and all heat transfer through cooling medium occurs by conduction. The volume of the coolant is modelled. Heat is removed from the system through internal and external walls. Heat flux condition is described by formula 3. In reality the lack of gas glow would be hard to achieve as the rotor is constantly rotating. It is a reference case for forced flow helium gas removal.
In the case of removal of heat with flowing helium gas the boundary condition on the boundaries facing the flow is described with formula

$$q_0 = h(T) \cdot (T_s - T) \tag{4}$$

where h is heat transfer coefficient and it is found based on definition of Nusselt number

$$h = \frac{Nu \cdot k_{He}}{D} \tag{5}$$

where D is characteristic dimension, assumed to be the same as the length of the rotor. Thermal conductivity of helium k_{He} is calculated based on data from [13]. Nu is calculated with formula based on [14]:

$$Nu = 0.916 \cdot Re^{0.5} \cdot Pr^{1/3} \tag{6}$$

where Re is Reynolds number found with equation

$$Re = \frac{\rho u L}{\mu} \tag{7}$$

where μ is dynamic viscosity, u is flow velocity and L is characteristic length, also assumed as the length of the rotor. Pr is Prandtl number calculated using formula

$$Pr = \frac{C_p \mu}{k} \tag{8}$$

It is assumed that the temperature-dependent properties of helium cooling the device are defined by the temperature of boundary layer, which is the same as the local temperature of a cooled boundary.
In the case of cooling with liquid nitrogen boundary condition at the cooled walls is also described with formula 4. h is calculated based on [15]:

$$h = \begin{cases} 21.945 \cdot \Delta T, & \text{when} \quad \Delta T < 4\ K \\ 82.74 - 131.22 \cdot \Delta T + 37.64 \cdot \Delta T^2 - 1.13 \cdot \Delta T^3, & \text{when} \quad 4\ K \leq \Delta T < 18.94\ K \\ 12292.13 - 709.32 \cdot \Delta T + 14.735 \cdot \Delta T^2 - 0.1061 \cdot \Delta T^3, & \text{when} \quad 18.94\ K \leq \Delta T < 56.3\ K \\ 120 + 0.069 \cdot \Delta T, & \text{when} \quad 56.3\ K \leq \Delta T < 214\ K \end{cases} \tag{9}$$

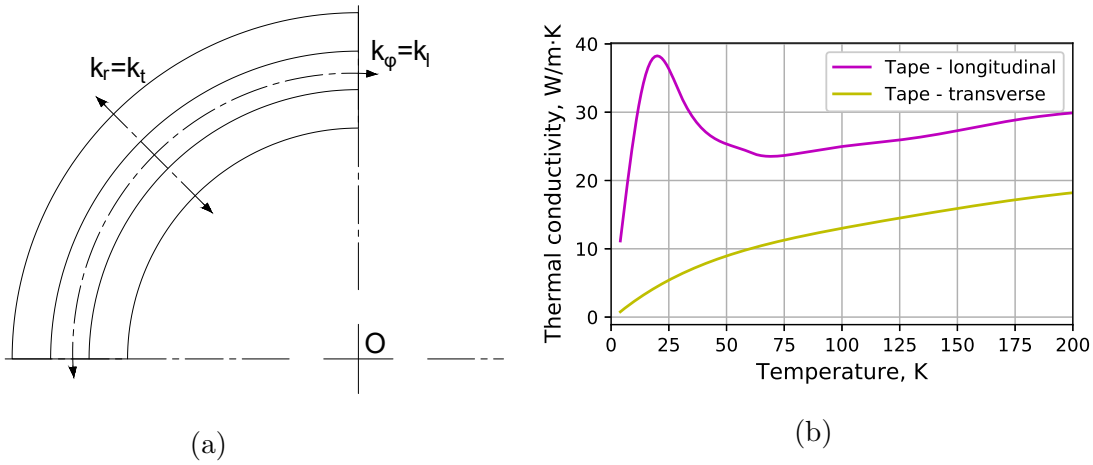

(a) (b)

Figure 2. Anistropy of thermal conductivity of a stack - (a) nomenclature of the geometry of the stack, (b) components of thermal conductivity

where ΔT is temperature difference between the cooling medium and the cooled object.
In every case heat source condition is applied at the half of the stack farther from the shaft. Heat generation is estimated as 5.2 W per stack during transient and 0.9 W during the stationary operation. In this paper the analysis is performed assuming the worst case scenario and maximum heat generation all the time. The losses in iron are very small and will be neglected.
The properties of stacks analysed in this paper are based on American Superconductor tape made without a copper coating, glued together with GE Varnish. Important aspect of heat transfer in stacks of superconducting stacks is their anisotropy. It comes from both the complex structure of the tapes forming it and on the stack arrangement itself. To account for that two coordinate systems were created for each stack and two components of thermal conductivity are considered, as shown in figure 2a [16]. The origin of each coordinate system is the same as the centre of a forming circle of the corresponding stack O.
In this case two components of thermal conductivity are radial k_r, which is the same as transverse thermal conductivity of the stack k_t, and angular k_ϕ, identical to longitudinal component k_l. The values of both components as the function of temperature are shown in figure 2b. Longitudinal thermal conductivity is significantly higher than transverse, therefore it can be expected that heat will be transferred along the stack to the thermal anchor. Anisotropy of properties tends to decrease with temperature, however in most of the temperature range remains a significant factor affecting heat transfer [16].
To account for the material and thermal anchoring method the thin layer condition is imposed on the boundaries between the stacks and the steel support, visible in figure 1. Its thickness is assumed as 100 μm to take into consideration possible misshape at the end of the stack which could be filled with mounting material. Two materials are considered, GE varnish and indium. Parameters of GE varnish are based on producer data and [17, 18]. The values for indium are fitted to experimental data from [19].

3. Results and Discussion

Figure 3a shows the dependence of maximum temperature of the stack on time in the case of conduction cooling in vacuum and cooling in stationary helium. Two methods of thermal anchoring are considered. The final temperature is obtained after long time, approximately 4000 s when the rotor is cooled in vacuum and 2000 s in the case of stationary helium cooling. Large increase of temperature occurs in both cases, approximately 40 K and 25 K respectively.

Such change leads to dramatic decrease of critical current density of the tapes of the stack. The trapped magnetic field is significantly decreased and so is the maximum power achievable by the motor.

The observed effect of the type of thermal anchor on the final temperature is slightly more

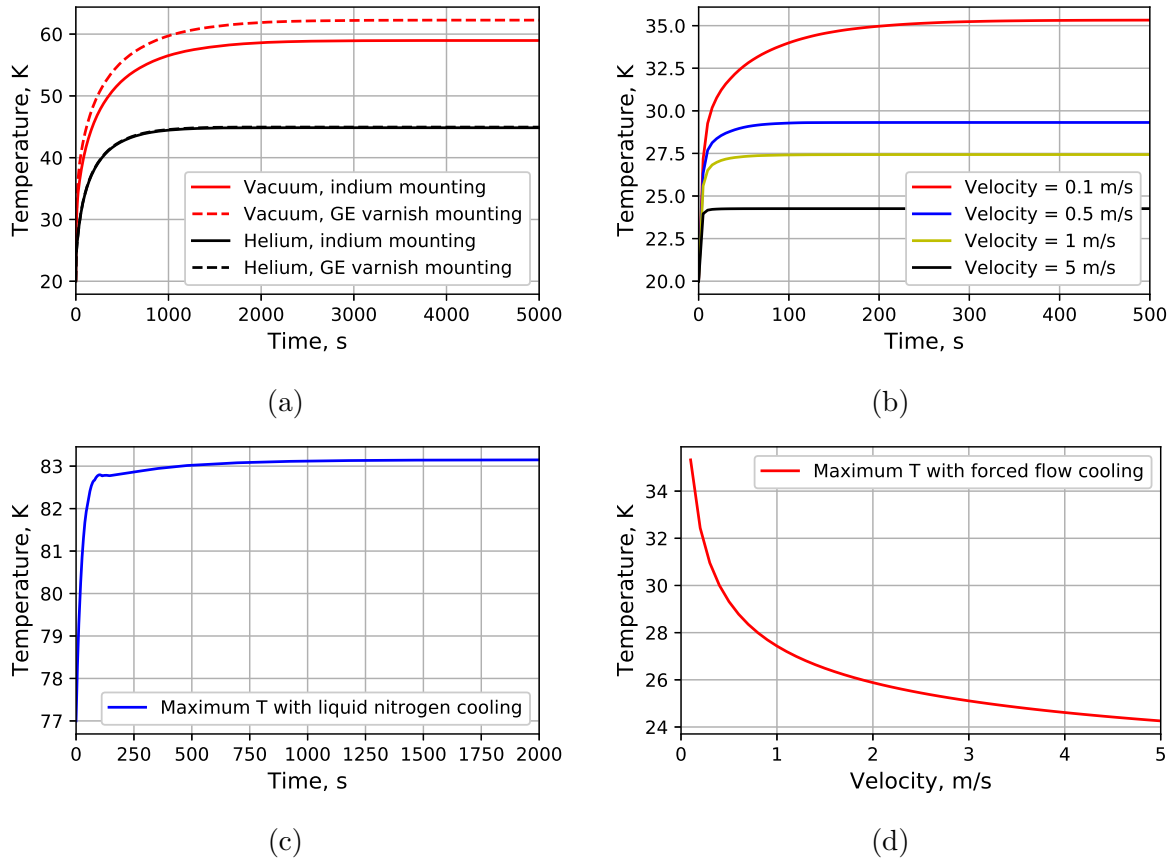

Figure 3. Dependence of maximum stack temperature on time for different cooling conditions - (a) conduction cooling in vacuum and stationary helium, (b) cooling by forced flow of gaseous helium with different velocities, (c) cooling with liquid nitrogen; (d) dependence of maximum temperature on forced flow velocity of helium

than 3 K for vacuum cooling. In the case of stationary helium conduction it is almost negligible. The majority of heat is transferred through the thermal anchor only in the case of cooling in vacuum, therefore the effect of the used material was expected to be strongest then. The results confirm this assumption and in any case other than vacuum cooling most of the heat is removed directly from the stack by a cooling medium.

Figure 3b shows the maximum temperature for forced convection cooling for different flow velocities. The final temperature is achieved in short time, decreasing with the increase of flow velocity. Temperature increase in every case is lower then for conduction cooling and also decreases with flow velocity. Maximum final temperature versus velocity is presented in figure 3d. It quickly decreases with the increase of velocity at its low values, then the curve flattens. The final value for high velocity flows is expected to be approximately 24 K. This cooling method seems to be most efficient choice.

Maximum temperature of stack cooled with liquid nitrogen is shown in figure 3c. The temperature changes are more complex than in previously considered cases. It rapidly increases

during first 100 s, achieving the value of 82.75 K. Then it slightly increases and after that start to slowly increase, achieving the final value of 83.1 K after 1500 s from the start. Such behaviour is due to rapid changes in heat transfer coefficient. Changes of boiling regime lead to dramatic changes of heat removal conditions.
Long time is required to obtain steady conditions, however temperature close to the final is achieved relatively quickly. With changing heat generation thermal instability of the device is possible. Sudden temperature increase can lead to the fast decrease of heat transfer coefficient and start positive feedback loop. Therefore, all possible changes of heat generation should be considered and a certain temperature difference must not be exceeded.

Figure 4a shows temperature distribution in steady state (the final state in figure 3a) for scenario with conduction cooling in vacuum. Large temperature differences can be seen between the tips of the stacks where most of heat is generated and the remaining parts of the rotor. All generated heat is transferred along the stack to the sink on the interior wall of the rotor. Poles are slightly warmer than interpoles, since their contact surface with the cooled wall is smaller.
Distribution of temperature when the rotor is cooled with stationary helium is presented in figure 4b (end of calculations in figure 3b). Temperature is much more homogeneous across the rotor than in the previous case. Part of heat is transferred through the gas to iron parts of the device and to the external wall, especially at the ends of the stacks. Iron has relatively high thermal conductivity and in the considered case the layer of gas actually serves as a semi-insulating barrier. Difference in temperature between poles and interpoles is very small.
Distributions of temperature with forced helium flow and boiling liquid nitrogen are shown in figures 4c and 4d respectively. Heat transfer patterns are very similar in both cases. Large part of heat is removed directly from the stacks to the surrounding medium. Still they are slightly warmer than the rest of the rotor. Temperature is even more homogeneous than in previous case, though. Temperature level is much higher when liquid nitrogen is applied as coolant. However, heat removal efficiency is similar in both cases as proved by low temperature difference between the stack and iron.
The results show that the best cooling method is forced flow cooling. It allows to achieve the lowest temperature change during the operation and is flexible. In the case of sudden increase of heat generation the flow of helium can be increased to improve heat transfer coefficient and heat extraction. The final temperature is achieved fast and any deviations from normal operation affecting heat generation can be quickly spotted. The major drawback is technical complexity of solution. Proper sealing is required to prevent helium from leaking out of the cryogenic system. In the final device the usage of liquid hydrogen is expected, which has additional benefit of high thermal capacity.
Conduction cooling methods are not sufficiently efficient. Temperature rise is much higher then with the application of other solutions. They cannot react quickly to sudden changes of heat input. Their heat extraction abilities could be enhanced by adding thermally conductive elements to the structure of the rotor. It would lead however to increased losses due to eddy current and potential decrease of mechanical strength of the machine. The major advantage of such solution is the lack of cryogen routing devices in the region of the rotor and the relative simplicity of a cryogenic system.
Nitrogen cooling offers very high heat transfer coefficient in certain conditions. Thanks to the latent heat of evaporation the cryogen is maintained at constant temperature. The drawback of this solution is the low stability in the case of sudden change of heat generation. This method cannot cool-down the stack below triple point of nitrogen. This limits the obtainable critical current density and electromagnetic efficiency of the stack. The temperature margin is much lower in this case. Additionally the expected friction losses would be high when compared to other methods.
Simulations show that the effect of the selected thermal anchor has very small effect on thermal

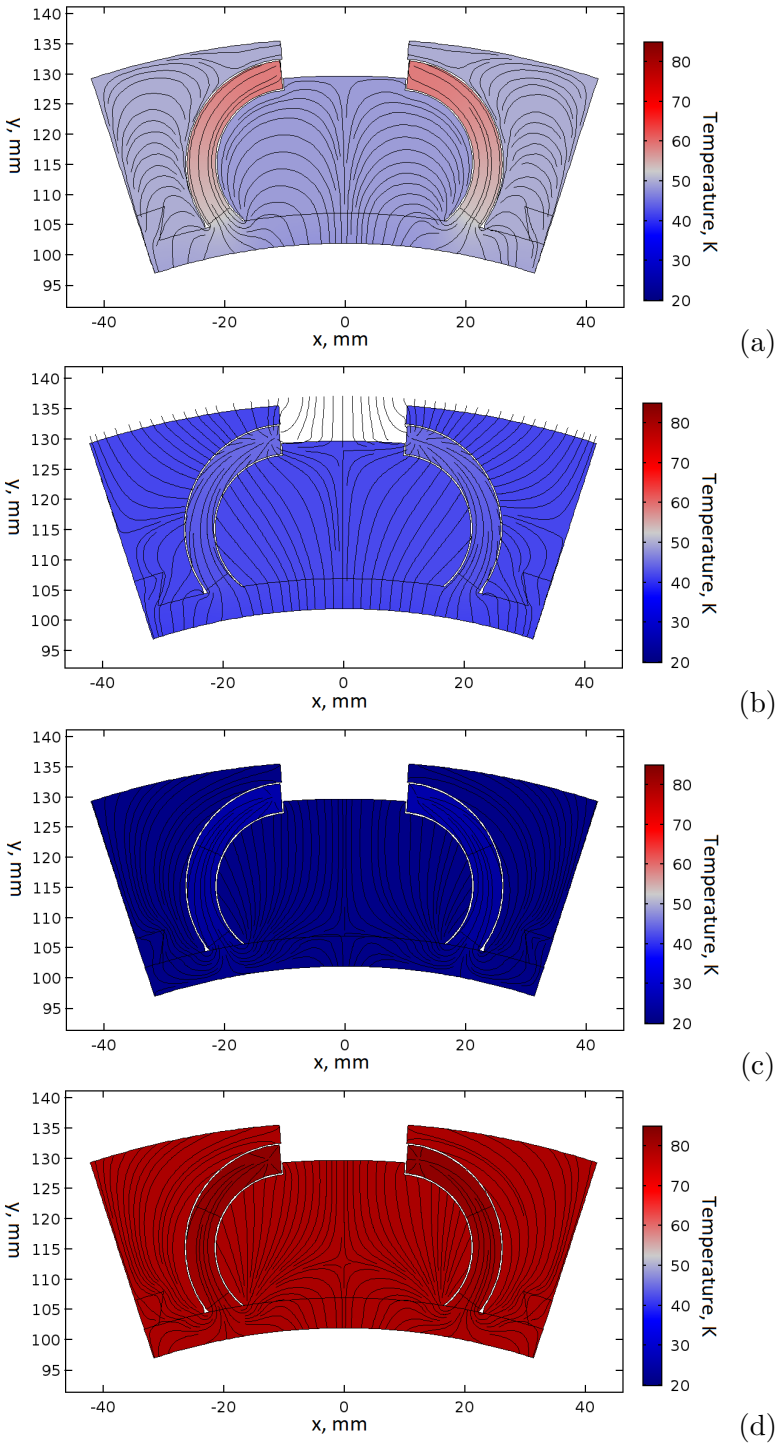

Figure 4. Distribution of temperature in steady-state for different cooling conditions - (a) conduction cooling in vacuum, (b) cooling with stationary helium, (c) cooling by forced flow of gaseous helium with velocity of 2.5 m/s, (d) cooling with liquid nitrogen

performance of the stack in most cases. Therefore glueing the stack to the surface seems to be better solution than soldering, as the generation of heat by eddy currents is much smaller. For most cooling methods majority of heat is removed directly from the surface of the stack.

Therefore any coating improving mechanical properties should have good thermal conductivity and allow for high heat transfer coefficients to ensure the safe operation of the stack.

4. Conclusions

The choice of cooling method is crucial for the efficient operation of the motor. Maintaining stack temperature at the lowest possible level maximises the trapped magnetic field and the achievable power of the motor. Temperature spikes contribute to demagnetisation and raise heat generation, possibly leading to a positive feedback loop and the complete loss of superconductivity. It also affects the mechanical design of the motor.

Among the considered methods the forced flow cooling is the most advantageous. It ensures the lowest temperature increase and allows to flexibly react to sudden changes of heat generation. It is more stable than liquid nitrogen cooling and allows to obtain significantly lower temperatures, depending on the cooling medium. Forced flow cooling is also much more efficient than conduction cooling in vacuum or cooling with a stationary gas.

Effect of thermal anchor is small for all cases except for conduction cooling in vacuum. In the remaining scenarios most of heat is directly transferred to the surrounding cryogen. It is important to consider it while designing the stack with exterior, potentially thermally insulating, layers. In the light of presented results the preferable anchoring method is glueing, as it limits heat generation due to eddy current. Future work will focus on experimental confirmation of findings and further search of methods for improvement of heat removal.

References

[1] Baskys A, Patel A, Hopkins S C, Kalitka V, Molodyk A and Glowacki B A 2015 *IEEE Transactions on Applied Superconductivity* **25** 1–4 ISSN 1051-8223

[2] Patel A, Baskys A, Mitchell-Williams T, McCaul A, Coniglio W, Hnisch J, Lao M and Glowacki B A 2018 *Superconductor Science and Technology* **31** 09LT01 URL https://doi.org/10.1088/2F1361-6668/2Faad34c

[3] Climente-Alarcon V, Patel A, Baskys A and Glowacki B A 2019 *IOP Conference Series: Materials Science and Engineering* **502** 012182 URL https://doi.org/10.1088/2F1757-899x/2F502/2F1/2F012182

[4] Bykovsky N, Uglietti D, Wesche R and Bruzzone P 2017 *Fusion Engineering and Design* **124** 6 – 9 ISSN 0920-3796 proceedings of the 29th Symposium on Fusion Technology (SOFT-29) Prague, Czech Republic, September 5-9, 2016 URL http://www.sciencedirect.com/science/article/pii/S0920379617304532

[5] Park M, Choi M, Hahn S, Cha G and Lee J 2004 *IEEE Transactions on Applied Superconductivity* **14** 1106–1109 ISSN 1051-8223

[6] Baskys A, Patel A and Glowacki B A 2018 *Superconductor Science and Technology* **31** 065011 URL https://doi.org/10.1088/2F1361-6668/2Faabf32

[7] Patel A, Climente-Alarcon V, Baskys A, Glowacki B A and Reis T 2018 Design considerations for fully superconducting synchronous motors aimed at future electric aircraft *2018 IEEE International Conference on Electrical Systems for Aircraft, Railway, Ship Propulsion and Road Vehicles International Transportation Electrification Conference (ESARS-ITEC)* pp 1–6

[8] Climente-Alarcon V, Smara A, Patel A, Glowacki B A, Baskys A and Reis T 2019 Field cooling magnetization and losses of an improved architecture of trapped-field superconducting rotor for aircraft applications *AIAA Propulsion and Energy Forum and Exposition, Indianapolis, Indiana* p 3189332

[9] Zou S, Zermeo V M R and Grilli F 2016 *IEEE Transactions on Applied Superconductivity* **26** 1–5 ISSN 1051-8223

[10] Song P, Qu T M, Lai L F, Wu M S, Yu X Y and Han Z 2016 *Superconductor Science and Technology* **29** 054007 URL https://doi.org/10.10882F0953-20482F292F52F054007

[11] Perez A, van der Woude R R and Dekker R 2019 *IOP Conference Series: Materials Science and Engineering* **502** 012139 URL https://doi.org/10.10882F1757-899x2F5022F12F012139

[12] Marquardt E, P Le J and Radebaugh R 2002 *Cryogenic Material Properties Database* pp 681–687

[13] Vargaftik N B and Yakush L V 1977 *Journal of engineering physics* **32** 530–532 ISSN 1573-871X URL https://doi.org/10.1007/BF00860600

[14] Liu Q S, Shibahara M and Fukuda K 2008 *Experimental Heat Transfer* **21** 206–219 (*Preprint* https://doi.org/10.1080/08916150802072859) URL https://doi.org/10.1080/08916150802072859

[15] Jin T, Hong J p, Zheng H, Tang K and Gan Z h 2009 *Journal of Zhejiang University-SCIENCE A* **10** 691–696 ISSN 1862-1775 URL https://doi.org/10.1631/jzus.A0820540

[16] Tomkow L, Mineev N, Smara A, Climente-Alarcon V and Glowacki B 2019 *Cryogenics* 103017 ISSN 0011-2275 URL http://www.sciencedirect.com/science/article/pii/S0011227519302589
[17] Jayasuriya K D, Stewart A M and Campbell S J 1982 *Journal of Physics E: Scientific Instruments* **15** 885–886 URL https://doi.org/10.1088/2F0022-3735/2F15/2F9/2F005
[18] Cude J and Finegold L 1971 *Cryogenics* **11** 394 – 395 ISSN 0011-2275 URL http://www.sciencedirect.com/science/article/pii/0011227571900397
[19] Ho C, Powell R and Liley P 1974 *J. Phys. Chem. Ref. Data, Suppl.* **3** 1–796